

MERIT Self-Directed Research

High-speed active metasurface modulator using III-V-on-insulator structure

Taichiro Fukui¹, Kei Sumita²

¹ Nakano and Tanemura Laboratory, Department of Electrical Engineering and Information Systems, School of Engineering, The University of Tokyo

² Takagi-Takenaka-Toprasertpong Laboratory, Department of Electrical Engineering and Information Systems, School of Engineering, The University of Tokyo

【About the Authors】

Taichiro Fukui: His research field is integrated photonics. In particular, he is currently working on optical phased arrays for optical sensing using the silicon photonics technology. In this joint research, he led the device design, numerical analysis, and characterization of the optical properties.

Kei Sumita: His research field is electronic devices. In particular, he is currently working on metal-oxide-semiconductor field-effect-transistors using III-V compound semiconductors and Ge for next generation logic circuits. In this joint research, he led the device fabrication and characterization of the electrical properties.

【Abstract】

Surface normal optical modulators are promising for various applications including optical communication and optical sensing due to its scalability to 2D arrays. On the other hand, it was difficult to realize high operation speed and high efficiency simultaneously due to the limited matter-light interaction due to short interaction time. In this work, we propose, design, and fabricate a surface normal optical modulator using InP thin film, which possess ideal characteristics of high electron mobility and small optical absorption. The proposed device comprises InP-based high-contrast grating which operates simultaneously as optical resonator and transparent electrode, and electro-optic polymer which is embedded in the high-contrast grating and will operate as the active material. From numerical analysis, we revealed that the proposed device can realize ultra-high operation speed feasible for optical communication. Furthermore, we fabricated a device and observed optical resonance at designed wavelength.

【Background】

Due to its feasibility of realizing 2D array, surface normal optical modulators are highly promising for many applications including massively parallel optical communication, optical wavefront modulation, and optical sensing. On the other hand, current surface normal optical modulators are based on either liquid crystal or MEMS, which strictly limits the operation speed of the device. Under such situation, Tanemura *et al.* proposed and demonstrated surface normal optical modulators using electro-optic polymers that can operate at a high speed [1] and silicon high-contrast grating [2] that enables high modulation efficiency [3,4].

Silicon high-contrast grating simultaneously play the role of optical resonator to enhance the modulation efficiency and the transparent electrode to apply voltage to the electro-optic polymer. Previously, high speed operation up to 500MHz is demonstrated, but further improvement in operation speed was required to leverage them in applications such as optical communication.

The operation speed of the device is limited by the RC time constant of the high-contrast grating. While the RC time constant can be improved by increasing the doping concentration of silicon, higher doping concentration will induce free-carrier absorption. When the doping concentration is too high, the absorption becomes a significant issue, and the high-contrast grating will not operate as an effective optical resonator. Thus, it is impossible to infinitely increase the doping concentration.

Compound semiconductors such as InP have much higher electron mobility compared to silicon and can realize much smaller electrical resistance at the same doping concentration. Moreover, thanks to the long scattering lifetime of carriers in compound semiconductors, they possess smaller optical absorption constant at the same doping concentration [5]. Thus, by replacing silicon with InP, the doping concentration and electron mobility can be improved simultaneously, and thus a drastic improvement in the electrical bandwidth of the device should be possible.

In order to fabricate a device consisting InP instead of silicon, InP-on-insulator structure that comprises InP thin film directly integrated on a low-refractive-index insulator substrate. However, it is difficult to access such substrate in the market and is also challenging to fabricate such structure. Takagi *et al.* have developed device fabrication technology of such III-V-on-insulator structures using direct wafer bonding method for electronic devices such as MOSFETs. Such fabrication technology is highly promising for realizing InP-based surface normal optical modulators.

【Research Aim】

In this work, we combine the surface-normal optical modulator technology of Tanemura-lab and device fabrication technology of Takagi-lab to realize ultra-high-speed surface normal optical modulators. By the collaboration of two students, we aim to demonstrate the device through numerical analysis and experiment.

【Device Design and Numerical Analysis】

In order to determine the structure of InP high-contrast grating, we performed electro-magnetic-field analysis based on finite-difference time-domain method (FDTD) using Lumerical (Ansys). At the first step, we ignored the optical absorption to determine the design center of the period and thickness of the high-contrast grating. Figure 1 shows the period and thickness dependence of the reflectance spectrum of the InP high-contrast grating as a color map. In this work, due to the applicability to optical communication and the abundant experiment infrastructure, we set the aimed operation wavelength to be 1550 nm. By further detailed numerical analysis, we determined the period of the grating to be 750 nm and thickness of

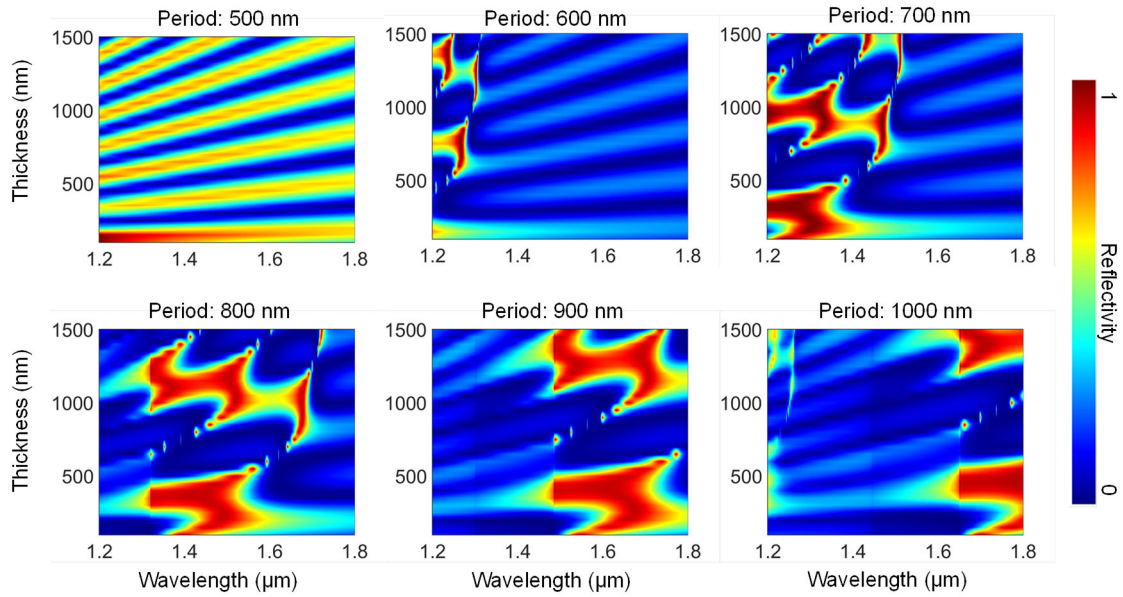


Fig. 1 Period and thickness dependency of the reflectance spectrum of the InP high-contrast grating

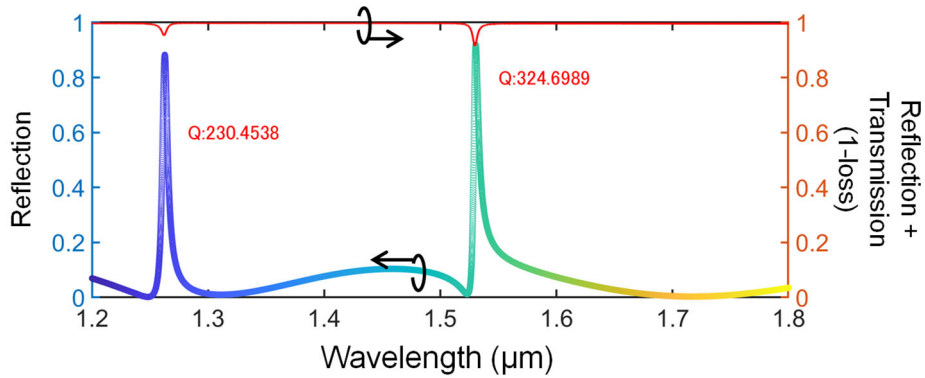


Fig. 2 Reflection spectrum of the InP high-contrast grating assuming that the doping concentration is $8 \times 10^{18} \text{ cm}^{-3}$. Note that there are two resonances: one near 1550 nm (fundamental mode), and another near 1250 nm (higher order mode). In this work, we make use of the fundamental mode.

the grating to be 600 nm.

Next, we calculated the impact of the optical absorption. After systematic numerical analysis, we have concluded that the grating can serve as a resonator even if the doping level is high as $1 \times 10^{19} \text{ cm}^{-3}$. As an example, in fig. 2, we show the reflection spectrum when the doping concentration is $8 \times 10^{18} \text{ cm}^{-3}$. Note that for the spectrum shown in Fig. 2, we have set the grating thickness to be 650 nm. This is because at the design center, the Q factor becomes extremely large ($Q > 3,000$) and the effect of optical absorption

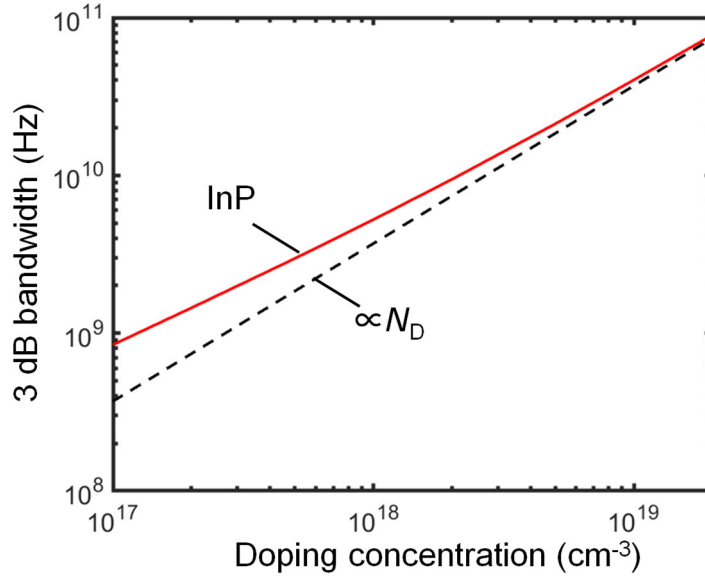


Fig. 3 Analysis of electrical bandwidth.

becomes serious, while in reality, the Q factor should be approximately several hundreds, due to the imperfection of the device and fabrication error. From Fig. 2, we can see that even at a relatively high Q factor of ~ 300 , the optical loss is limited to $\sim 10\%$. Note that higher Q factor leads to higher modulation efficiency, but the optical bandwidth of the device will become limited if the Q factor is too high. Thus, a moderately high Q factor of $10\sim 1000$ is believed to be appropriate [7].

We then numerically simulated the electrical bandwidth of the device. Figure 3 shows the doping concentration dependency of the 3 dB bandwidth of the device. Here we assumed the device size to be $40\ \mu\text{m} \times 40\ \mu\text{m}$. The RC time constant can be reduced by making the device size smaller. However, since the finite size effect will become prominent for the optical property if the device size becomes too small, we cannot infinitely scale down the device. The size chosen here is based on past study so that it is feasible to operate as a resonator. From the frequency dependency, the 3 dB bandwidth was derived to be 40 GHz when the doping concentration is $10^{19}\ \text{cm}^{-3}$, which is fast enough to be used even in high-speed applications including optical communication.

[Device Fabrication and Evaluation]

We have fabricated the designed device based on the fabrication flow shown in Fig. 4. First, we epitaxially grew InGaAs/InP layers on InP substrate by metal organic vapor phase epitaxy. Here, the device layer was set to be 600 nm based on the device design, and the sacrificial InP and InGaAs layers were set to be $50\sim 100$ nm based on previous work [6]. We show the scanning electron microscopic image of the grown substrate in Fig. 5(a). After wafer cleaning, deposition of Al_2O_3 bonding layer, and degassing process, the InP wafer was directly bonded on a quartz substrate. The wafer after the bonding procedure is shown in Fig. 5(b). Successively, we improved the bonding strength by inducing high pressure to the substrate, and removed

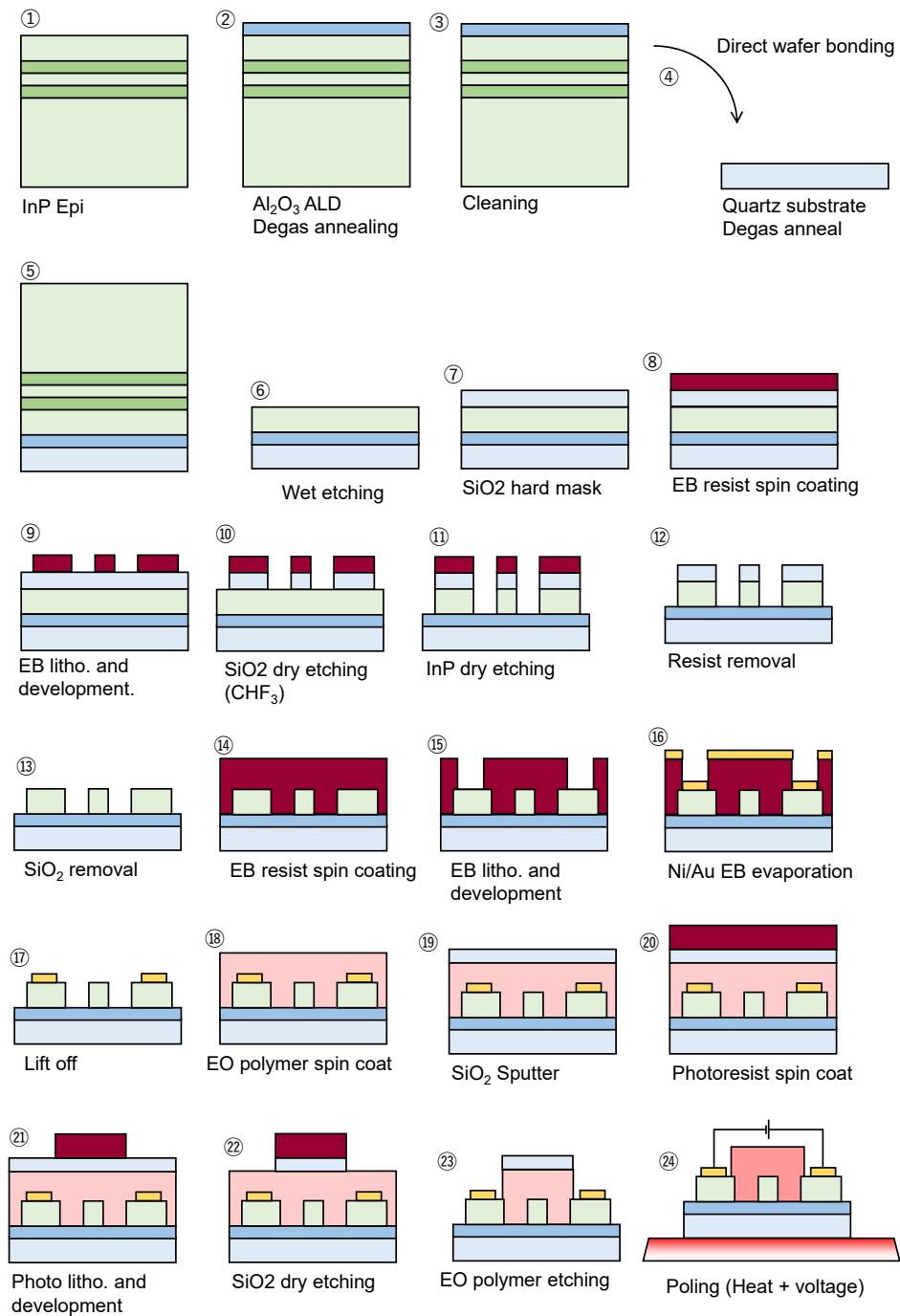


Fig. 4 Fabrication flow of the device.

the sacrificial layers by wet etching to form a thin film. Next, we deposited SiO_2 as hard mask, performed electron beam lithography, and performed dry etching of InP. Here, the sidewall angle becomes an critical issue for the device property, but by conditioning, we have found a condition to realize a vertical sidewall [Fig. 5(c)]. We then formed the contact electrode by electron beam lithography and lift off. Figure 5(d) shows the microscopic image of the device after electrode formation. Successively, we spin coated electro-

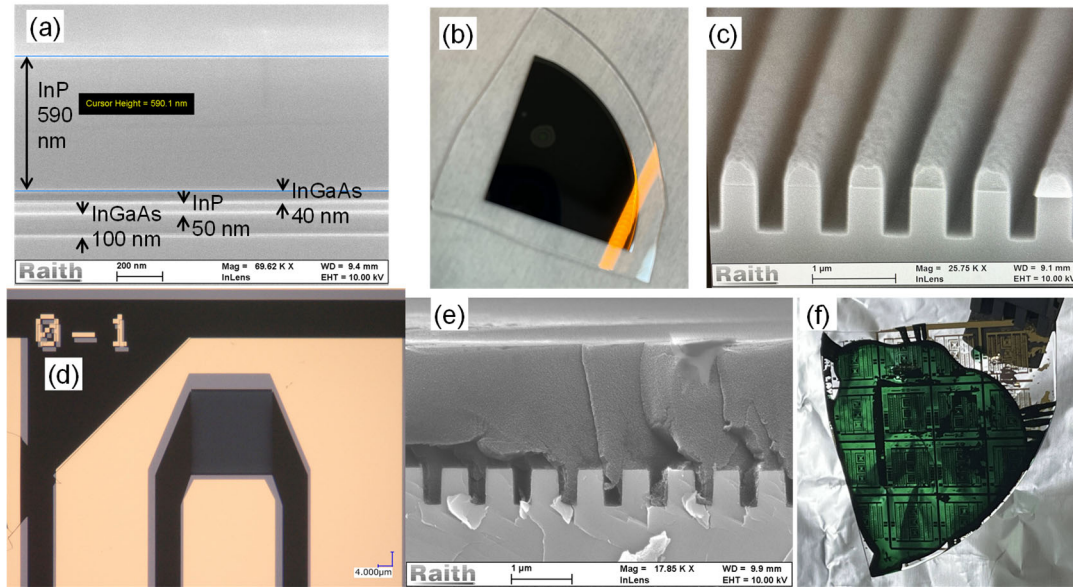


Fig. 5 (a) Scanning electron microscopic image of the epitaxial wafer. (b) Photograph of wafer after the direct wafer bonding process. (c) Cross sectional scanning electron microscope image of the InP dummy substrate after dry etching conditioning process. (d) Microscope image after the electrode formation. (e) Cross sectional scanning electron microscope image of the dummy InP substrate after electro-optic polymer spin coating. (f) Photograph of the chip after electro-optic polymer spin coating.

optic polymer. Here, it is critically important for the device performance to have the electro-optic polymer embedded perfectly in the high-contrast grating. We also have performed conditioning here and have confirmed that the polymer can be embedded without any problem, as shown in Fig. 5(e). A photography of the device after spin coating of the polymer is depicted in Fig. 5(f). After spin coating, we deposited SiO_2 , performed photo lithography, and removed unnecessary electro-optic polymer so that we can take contact to the electrode. Currently, we are working on wire bonding of the device and poling of the electro-optic polymer.

We evaluated the static performance of the device, although we could not accomplish evaluation of the active performance due to the limitation in time. First, the electrical property of the device is evaluated by transmission line model (TLM) method. The measured electrical resistance of the InP thin film is shown in Fig. 6. From here, the contact resistance and the resistivity were measured to be $2.68 \Omega\text{cm}^{-2}$ and $0.0011 \Omega\text{cm}$, respectively. The contact resistance was in good agreement with previous work [8,9]. Assuming the doping concentration to be $8 \times 10^{18} \text{cm}^{-3}$, which we measured at the conditioning step using CV method, the mobility was measured to be $700 \text{cm}^2/\text{Vs}$. This is also in good agreement with the literature [10]. Note that this resistivity is 25 times lower than silicon with 10^{18}cm^{-3} doping concentration, which was used in the previous work. Finally, we evaluated the optical property of the high-contrast grating. We show an example of the reflectance spectrum in Fig. 7. As designed, a resonance is obtained at 1550 nm wavelength. Here,

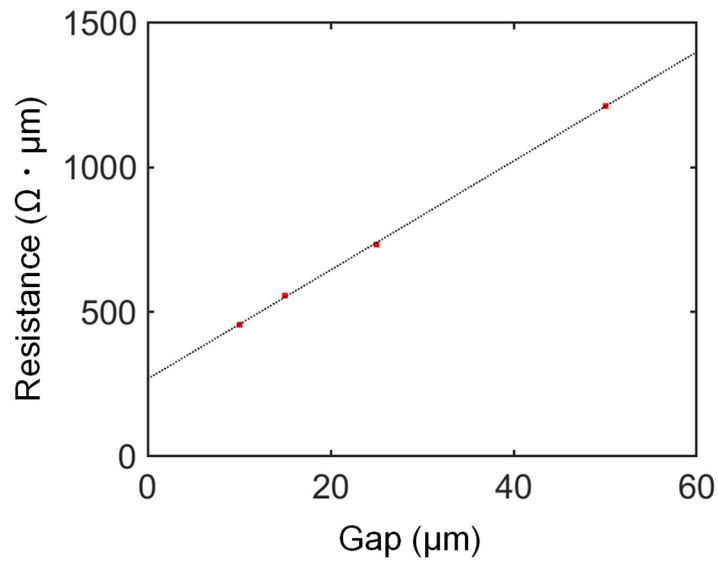


Fig. 6 Measurement result of TLM method.

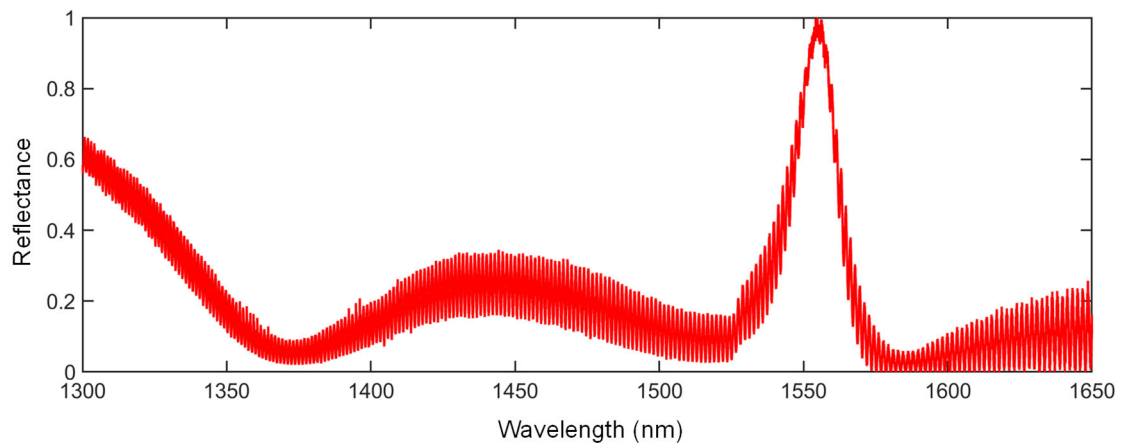


Fig. 7 Reflectance spectrum of the fabricated device.

the small resonance observed as a background is probably induced by the Fabry-Perot resonance of the quartz substrate. The Q factor was ~ 75 . The reason of the relatively low Q factor compared to the design is still unclear. However, even with such moderate Q factor, efficient modulation should be possible by using a high-performance electro-optic polymer [11]. In fact, broad band operation should be possible due to the relatively low Q factor. From the high peak reflectance at the resonance, we can see that we simultaneously realized low electrical resistance and small optical absorption that does not degrade the optical resonance. We will further pursue the demonstration of high-speed operation.

【Acknowledgement】

First of all, we would like to express our sincerely gratitude to our supervisors, Prof. Shinichi Takagi and Prof. Takuo Tanemura for their continuous support, supervision, and encouragement through the project.

At the same time, we would like to thank our co-advisors, Prof. Yoshiaki Nakano, Prof. Masakazu Sugiyama, Prof. Mitsuru Takenaka, and Dr. Kasidit Toprasertpong for their support in various aspect of this research, from providing the experiment infrastructures to detailed technical advises. We thank our assistant supervisors, Prof. Toshiro Hiramoto and Prof. Ryo Shimano, for supporting and encouraging this joint-research, and for providing us insightful comments from various point of views. We thank Dr. Warakorn Yanwachirakul for his support in epitaxial growth of InP/InGaAs substrate, Mr. Go Soma and Mr. Hiroki Miyano for their support in Electron Beam lithography, Mr. Ryota Tanomura for his support in dry etching, and Mr. Jiahao Liu for his support in spin coating of electro-optic polymer. Finally, we would like to thank Material Education program for the future leaders in Research, Industry, and Technology (MERIT) for providing us the opportunity of this productive joint-research and for their massive financial support through the Ph.D. program.

【References】

- [1] C. J. Chang-Hasnain and W. Yang, *Adv. Opt. Photon.* **4**(3), 379 (2012).
- [2] D. Chen *et al.* *Appl. Phys. Lett.* **70**(25), 3335 (1997).
- [3] Y. Kosugi *et al.*, *IEICE Electron. Express* **13**(17), 20160595 (2016).
- [4] M. Ogasawara *et al.*, *CLEO'19*, JTH2A.48.
- [5] N. Sekine *et al.*, *Opt. Express* **28**(20), 29730 (2020).
- [6] M. Yokoyama *et al.*, *IEEE Electron Dev. Lett.* **32**(9), 1218 (2011).
- [7] D. A. B. Miller, *J. Lightw. Technol.* **35**(3), 346 (2017).
- [8] S.-H. Kim *et al.*, *Appl. Phys. Lett.* **98**(24), 243501 (2011).
- [9] A. Baraskar *et al.*, *J. Appl. Phys.* **114**(15), 154516 (2013).
- [10] M. Sotoodeh *et al.*, *J. Appl. Phys.* **87**(6), 2890 (2000).
- [11] H. Xu *et al.*, *Adv. Mater.*, **33**(45), 2104174 (2021).